The Ca^{2+}-Dependent Interaction of S100B($\beta\beta$) with a Peptide Derived from p53[†]

Richard R. Rustandi, Alexander C. Drohat, Donna M. Baldisseri, Paul T. Wilder, and David J. Weber*

Department of Biochemistry and Molecular Biology, University of Maryland School of Medicine, Baltimore, Maryland 21201

Received October 30, 1997; Revised Manuscript Received December 17, 1997

ABSTRACT: S100B($\beta\beta$) was found to interact with the tumor suppressor protein, p53, and inhibit its PKC-dependent phosphorylation and tetramer formation [Baudier, J., Delphin, C., Grunwald, D., Khochbin, S., and Lawrence, J. J. (1992) *Proc. Natl. Acad. Sci. U.S.A. 89*, 11627−11631]. Since PKC-dependent phosphorylation at the C-terminus of p53 is known to effect transcription and p53 tetramer formation [Sakaguchi, K., Sakamoto, H., Lewis, M. S., Anderson, C. W., Erickson, J. W., Appella, E., and Xie, D. (1997) *Biochemistry 36*, 10117−10124], we examined the interaction of S100B($\beta\beta$) with a peptide derived from the C-terminal regulatory domain of p53 (residues 367−388). In this paper, we report that S100B($\beta\beta$) binds to the p53 peptide ($^{Ca}K_3 \leq 23.5 \pm 6.6\ \mu$M) in a Ca^{2+}-dependent manner, and that the presence of the p53 peptide was found to increase the binding affinity of Ca^{2+} to S100B($\beta\beta$) by 3-fold using EPR and PRR methods, whereas the peptide had no effect on Zn^{2+} binding to S100B($\beta\beta$). Fluorescence and NMR spectroscopy experiments show that the p53 peptide binds to a region of S100B($\beta\beta$) that probably includes residues in the "hinge" (S41, L44, E45, E46, I47), C-terminal loop (A83, C84, H85, E86, F87, F88), and helix 3 (V52, V53, V56, T59). Together these data support the notion that S100B($\beta\beta$) inhibits PKC-dependent phosphorylation by binding directly to the C-terminus of p53.

The S100 protein family is a highly conserved group of Ca^{2+}-binding proteins with molecular masses ranging from 10 to 12 kDa. The principal member of the S100 family, S100B, was first discovered as a major constituent of glia (*2*); however, it is now known to be expressed in several tissues and cell lines including malignant tumors (*3*−*6*).[1] Sequencing studies demonstrated that S100B exists either as a heterodimer with S100A1, S100($\alpha\beta$), or as a homodimer (*5*). The homodimeric form of S100B has either a disulfide bond at the dimer interface, S100B($\beta_{S-S}\beta$), or its cysteine residues are reduced, S100B($\beta\beta$). While the precise mechanisms for intra- and extracellular functions of S100B are not well understood, processes such as neurite extension, Ca^{2+}-flux, cell growth, apoptosis, energy metabolism, and protein phosphorylation are all thought to be modulated in some manner by S100B (*5*−*8*).

The reduced homodimeric protein, S100B($\beta\beta$), is one of the best characterized proteins of the S100 family. The solution structure of reduced apo-S100B($\beta\beta$) shows that two subunits associate tightly (K_D < 500 pM) (*9*) through extensive hydrophobic interactions to form a compact dimer with a highly charged surface (*10*−*12*). Characteristic of all S100 proteins, the first helix−loop−helix Ca^{2+}-binding domain of each S100β subunit (residues 18−31) has 2 more amino acid residues than typical EF-hands (14 versus 12 residues). Furthermore, several of the Ca^{2+}-liganding residues of the S100-hand (or pseudo-EF-hand) do not conform to those of the EF-hand consensus sequence (*13*, *14*). As a result, the pseudo-EF-hand binds Ca^{2+} with a very low affinity ($K_D = 200-500\ \mu$M) (*15*) whereas the second Ca^{2+}-binding domain (residues 61−72) contains the consensus EF-hand sequence (*7*, *12*−*14*) and binds Ca^{2+} with a relatively high affinity ($K_D = 20-50\ \mu$M) (*7*, *15*). The two EF-hand domains of S100B($\beta\beta$) are connected by a loop which is often referred to as the "hinge" region. Interestingly, the hinge and C-terminus have little sequence homology in the S100 family, and together these regions are thought to be important for specific interactions between S100 proteins and their respective targets (*5*, *7*, *9*, *10*).

The general model for S100−target protein interactions is similar to that of other Ca^{2+}-binding proteins such as calmodulin and troponin C. As for these proteins, S100B($\beta\beta$) undergoes a conformational change upon binding Ca^{2+} that promotes its interaction with a variety of target proteins (*7*, *10*, *16*). For example, the Ca^{2+}-dependent binding of S100B($\beta\beta$) to microtubules (*17*), GFAP (*18*),[1] and p53 (19) prevents oligomerization for each of these proteins. Fur-

[†] This work was supported by grants from the National Institutes of Health (Grant R29GM52071 to D.J.W.), the American Cancer Society (Grant JFRA-641 to D.J.W.), the University of Maryland School of Medicine, and SRIS/DRIF funding from the State of Maryland (to D.J.W.). The 600 MHz NMR spectrometer at the UMB NMR facility was purchased with funds from the University of Maryland and the NIH shared instrumentation grant program (S10RR10441 to D.J.W.).

* To whom correspondence should be addressed. Phone: (410) 706-4354. FAX: (410) 706-0458. Email: weber@noe.ab.umd.edu.

[1] Abbreviations: PKC, protein kinase C; PSCBD, phosphorylation site/calmodulin binding domain; GFAP, glial fibrillary acidic protein; MARCKS, myristoylated alanine-rich C kinase substrate; SMP, S-100 modulated phosphoprotein; DTT, dithiothreitol; βME, β-mercaptoethanol; IC, inhibition constant; BCA, bicinchoninic acid; EPR, electron paramagnetic resonance; PRR, proton relaxation rate; TPPI, time proportion phase incrementation; DIPSI-2rc, decoupling in the presence of scalar interaction version 2rc; HSQC, heteronuclear single-quantum coherence; NOE, nuclear Overhauser effect; NOESY, nuclear Overhauser effect spectroscopy; TOCSY, total correlation spectroscopy; HOHAHA, homonuclear Hartman−Hahn spectroscopy; HMQC, heteronuclear multiple quantum coherence; CBCA(CO)NH, β- and α-carbon to nitrogen (via carbonyl) to amide proton correlation; TSP, sodium 3-(trimethylsilyl)propionate-*2,2,3,3-d*$_4$; p53, tumor suppresor protein; S100β, a subunit of dimeric S100B($\beta\beta$); S100B($\beta\beta$), dimeric S100B with noncovalent interaction at the dimer interface.

S0006-2960(97)02701-3 CCC: $15.00
Published on Web 01/30/1998

thermore, S100B($\beta\beta$) inhibits the PKC-dependent phosphorylation of τ-protein (*20*), neuromodulin (*21*, *22*), SMP (*23*), MARCKS (*24*), and p53 (*19*, *25*, *26*) by binding to the phosphorylation site of these PKC substrates.

To further characterize the interaction of S100B($\beta\beta$) with target proteins, we examined the interaction of S100B($\beta\beta$) with a peptide derived from the tumor suppressor protein, p53. Previously, Baudier and co-workers showed that full-length p53 is a substrate for PKC in vivo and in vitro, and that S100B($\beta\beta$) interacts with p53 to inhibit phosphorylation and p53 tetramer formation (*19*). Recently, phosphorylation at the C-terminus of p53 was shown to directly affect the ability of p53 to form tetramers and subsequently activate transcription (*27*, *28*). Furthermore, monoclonal antibodies engineered to bind the C-terminal regulatory domain of p53 (residues 369−383) were found to activate the function of p53 as a specific transcription factor in a manner similar to cells treated with UV radiation (*29*). Therefore, it is important to determine whether the S100B($\beta\beta$) binding site on p53 is in its C-terminal regulatory domain.

As for full-length p53 (*19*), we found that a 22 residue peptide derived from the C-terminus of p53 (residues 367−388) is a good substrate for PKC, and that its PKC-dependent phosphorylation is inhibited by S100B($\beta\beta$) in a Ca^{2+}-dependent manner (*25*, *26*). In this paper, peptide-binding studies show for the first time that a Ca^{2+}-dependent interaction between p53 and S100B($\beta\beta$) occurs at the C-terminus of p53, and that this interaction explains the inhibition kinetics observed by Wilder et al. 1997 (*26*). Furthermore, the interaction between S100B($\beta\beta$) and the p53 peptide was found to increase the Ca^{2+}-binding affinity of S100B($\beta\beta$) by 3-fold. Finally, ^{1}H and ^{15}N chemical shift values for residues from the hinge region (S41, L44, E45, E46, I47), the C-terminal loop (A83, C84, H85, E86, F87, F88), and helix 3 (V52, V53, V56, T59) of S100B($\beta\beta$) are most affected by peptide binding likely because they are at the p53 peptide−S100B($\beta\beta$) interface.

EXPERIMENTAL PROCEDURES

Materials. All chemical reagents were ACS grade or higher and purchased from Sigma unless otherwise indicated. All buffers were passed through Chelex-100 resin (Bio-Rad) to remove trace metals. Perdeuterated Tris, Tris-d_{11} (1 M solution in D_2O, >98.7 atom % deuterium), was purchased from C/D/N Isotopes, Inc. (Vandreuil, Quebec) D_2O (100.0 atom % deuterium, low in paramagnetic impurities) was purchased from Aldrich Chemical Co. (Milwaukee, WI). $^{15}NH_4Cl$ (>99%) and ^{13}C-labeled glucose were purchased from Cambridge Isotope Laboratories (Woburn, MA).

S100B($\beta\beta$) and p53-Derived Peptide Preparations. Recombinant S100B($\beta\beta$) was overexpressed in *E. coli* strain HMS174(DE3) transformed with an expression plasmid containing the rat S100β gene. Unlabeled, ^{15}N-labeled, and ^{13}C,^{15}N-labeled S100B($\beta\beta$) were prepared and purified (>99%) under reducing conditions using procedures similar to those described previously (*10*, *12*), except that 0.5 mM DTT (Gibco BRL) was used as a reducing agent throughout the preparation instead of β-mercaptoethanol. The S100β subunit concentration was determined using a BCA protein assay with S100B($\beta\beta$) of known concentration as the standard (*9*, *10*, *12*). The concentration of standard S100β used in the BCA assay was determined by amino acid analysis (Analytical Biotechnology Services, Boston, MA).

A peptide, acetyl-SHLKSKKGQSTSRHKKLMFKTE-am, derived from human p53 (residues 367−388) was synthesized using solid-phase peptide synthesis (Biopolymer Laboratory, University of Maryland School of Medicine at Baltimore, MD) with its N- and C-termini acetylated (acetyl-) and amidated (-am), respectively. The p53 peptide was stored as a lyophilized powder, and dissolved in 1 mM Tris-HCl-d_{11}, pH 7.6, prior to use. The purity (>99%) of the p53 peptide was determined using HPLC, and its concentration and composition were confirmed by amino acid analysis (Analytical Biotechnology Services). A second peptide was synthesized with a tryptophan at position 385 rather than a phenylalanine (F385W p53 peptide), acetyl-SHLKSKKGQSTSRHKKLMWKTE-am. For fluorescence spectroscopy experiments, the F385W p53 peptide was further purified with an additional G-15 Sephadex (Pharmacia) gel permeation column (0.9 × 28 cm) in 25 mM Tris-HCl and 50 mM NaCl, pH 7.6. The concentration of the F385W p53 peptide was determined at neutral pH using an extinction coefficient $\epsilon_{280} = 5600\ cm^{-1}\ M^{-1}$ as for the methyl ester of *N*-acetyltryptophan (*30*).

Fluorescence Spectroscopy. All fluorescence spectra were collected on a SLM-Aminco series 2 fluorescence spectrophotometer with the temperature of the cell maintained at 22 °C using a circulating constant-temperature bath. The measurements were done in a quartz cuvette with 0.2 and 1 cm excitation and emission path lengths, respectively. The excitation wavelength was set to 295 nm, and the excitation slit width was 4 nm. The emission was scanned from 300 to 550 nm to determine the emission wavelength maxima for the F385W p53 peptide with a slit width of 4 nm. The binding of S100B($\beta\beta$) to the F385W p53 peptide was monitored by an increase in fluorescence intensity at 338 nm during titrations of S100B($\beta\beta$) into a solution of the F385W p53 peptide (14 μM). All measurements were performed in 6 mM $CaCl_2$, 25 mM Tris-HCl, 6 mM NaCl, 2 mM DTT, pH 7.6, buffer. Data for the F385W p53 peptide binding to the S100B($\beta\beta$)−Ca^{2+} complex ($^{p53F385W-Ca}K_3$) were fit to a single site binding model with one peptide bound per S100β subunit. The dissociation constant for the wild-type p53 peptide was obtained by competition experiments in which the corresponding S100B($\beta\beta$)−Ca^{2+}−F385W p53 peptide complex was titrated with wild-type p53 peptide, monitoring the displacement of the F385W p53 peptide by an observed decrease in fluorescence intensity at 350 nm. In this case, the change in fluorescence intensity was best fit to the Hill equation to give the upper limit for the apparent dissociation constant (K_{app}) and a Hill coefficient $n_H = 3.2 \pm 0.8$.[2] The upper limit for the actual dissociation ($^{Ca}K_3$) of the wild-type p53 peptide from the S100B($\beta\beta$)−Ca^{2+}−p53 peptide complex was calculated using $^{Ca}K_3 = K_{app}/(1 +$

[2] At this point, it is not completely clear why there is a sigmoidal binding curve observed for the wild-type p53 peptide. This can be due to cooperative binding and/or due to a very slow kinetic step(s) of binding (>30 min) that occurs at low p53 peptide concentrations. As a result, upper limit K_3 values are reported (Table 2) for the wild-type peptide in both the Mn^{2+} and Ca^{2+} complexes. Furthermore, cooperative p53 peptide binding is a less likely explanation since preliminary results which monitored observed off-rates of Ca^{2+} as a function of p53 concentration have no sigmoidal shape and give a $^{p53peptide}K_{1/2} = 3 \pm 2\ \mu M$.

Table 1: Parameters for NMR Experiments[a]

		parameters[b]			
experiment	dim	nucl	time pts	freq pts	acq time (ms)
2D ^{1}H,^{15}N−HSQC	t_1	^{15}N	128	256	52.6
	t_2	^{1}H	512	1024	61.1
2D NOESY[c]	t_1	^{1}H	512	2048	61.1
	t_2	^{1}H	512	2048	61.1
2D TOCSY[d]	t_1	^{1}H	512	2048	61.1
	t_2	^{1}H	512	2048	61.1
3D ^{15}N-edited NOESY−HSQC[c]	t_1	^{1}H	106	256	10.7
	t_2	^{15}N	28	64	11.5
	t_3	^{1}H	512	1024	61.1
3D ^{15}N-edited HOHAHA-HSQC[e]	t_1	^{1}H	90	256	10.7
	t_2	^{15}N	24	64	9.9
	t_3	^{1}H	512	1024	61.1
3D ^{15}N,^{15}N-edited HMQC−NOESY−HSQC[f]	t_1	^{15}N	42	64	8.6
	t_2	^{15}N	42	64	8.6
	t_3	^{1}H	512	1024	61.1
3D ^{13}C-edited HMQC−NOESY[c]	t_1	^{1}H	115	512	13.7
	t_2	^{13}C	60	128	13.3
	t_3	^{1}H	512	1024	61.1
3D HCCH-TOCSY[g]	t_1	^{1}H	128	512	15.2
	t_2	^{13}C	48	128	8.0
	t_3	^{1}H	512	1024	61.1
3D CBCA(CO)NH[h]	t_1	^{13}C	140	256	11.6
	t_2	^{15}N	32	64	23.9
	t_3	^{1}H	512	1024	61.1
3D HNCACB	t_1	^{15}N	22	64	16.4
	t_2	^{13}C[l]	64	128	7.1
	t_3	^{1}H	512	1024	61.1
4D ^{13}C,^{15}N-edited NOESY−HSQC[c]	t_1	^{13}C	19	64	5.3
	t_2	^{1}H[i]	64	128	12.5
	t_3	^{15}N	13	64	10.2
	t_4	^{1}H[j]	256	512	35.6
4D ^{13}C,^{13}C-edited NOESY−HSQC[c]	t_1	^{13}C[k]	18	64	5.0
	t_2	^{1}H	64	128	11.1
	t_3	^{13}C[k]	18	32	5.0
	t_4	^{1}H	256	1024	35.6

[a] Data were collected in H_2O at 37 °C at 600.13 MHz for ^{1}H. [b] Number of points in the time domain is complex. Number of points in the frequency domain is real. The carrier frequencies were 4.658, 40.6, and 118.9 ppm for ^{1}H, ^{13}C, and ^{15}N nuclei, respectively, unless otherwise noted. [c] The NOE mixing time was 100 ms. [d] The TOCSY spin-lock time was 70 ms using a 10 kHz rf field strength and a MLEV-17 mixing sequence. [e] The HOHAHA spin-lock time was 70 ms using a 10 kHz rf field strength and a relaxation-compensated DIPSI-2 mixing sequence. [f] The NOE mixing time was 150 ms. [g] The TOCSY spin-lock duration was 22.9 ms using a DIPSI-2 mixing sequence and 7 kHz rf field strength. The ^{13}C carrier position was 45.2 ppm. [h] The ^{13}C carrier position was 48.2 ppm. [i] The ^{1}H carrier position was 3.9 ppm. [j] The ^{1}H carrier position was 8.70 ppm. [k] The ^{13}C transmitter was set to 68.6 ppm. [l] The ^{13}C carrier was 45.6 ppm.

([F385W p53 peptide]/$^{p53F385W-Ca}K_3$)), and this value for $^{Ca}K_3$ did not increase when other competition equations that included cooperative effects were considered. For all titrations, the fluorescence emission spectra were corrected for the presence of S100B($\beta\beta$) (<5% corrections) and dilution factors (<5% correction). In the competition studies, corrections for wild-type p53 peptide (<2% corrections) were also applied.

NMR Spectroscopy. Table 1 lists the NMR experiments necessary to sequence-specifically-assign S100B($\beta\beta$) in the S100B($\beta\beta$)−Ca^{2+}−p53 peptide complex. Heteronuclear NMR spectra were collected at 37 °C with a Bruker DMX600 NMR spectrometer (600.13 MHz for protons) equipped with four frequency channels and a triple-resonance three-axis gradient probe. Unless otherwise stated, a 1 s relaxation delay was used, and quadrature detection in the indirect dimensions was obtained with States-TPPI phase cycling (*31*). For most experiments, initial delays in the indirect dimensions were set to give zero- and first-order phase corrections of 90° and −180°, respectively (*32*). Data were processed on Silicon Graphics workstations using the processing program nmrPipe (*33*). Time-domain data in the indirect dimensions were extended by no more than one-third using standard linear prediction routines (*34*), except for data in constant time domains which were extended 2-fold using mirror-image linear prediction (*35*). All proton chemical shifts are reported with respect to the H_2O or HDO signal taken as 4.658 ppm relative to external TSP (0.0 ppm) at 37 °C. The ^{13}C and ^{15}N chemical shifts were indirectly referenced using the following ratios of the zero-point frequencies at 37 °C: 0.10132905 for ^{15}N to ^{1}H and 0.25144953 for ^{13}C to ^{1}H (*36*−*38*).

All NMR samples contained 3.0−3.3 mM S100β (subunit concentration), 0.1 mM EDTA, 0.34 mM NaN_3, 5 mM DTT, 17 mM NaCl, 10 mM Tris-HCl-d_{11}, 10% D_2O, 6.3 mM $CaCl_2$, pH 6.5. The p53 peptide was lyophilized and redissolved as a stock solution (60.5 mM) in 1 mM Tris-HCl-d_{11}. The pH of the stock solution was adjusted to 6.5 with cold dilute HCl prior to adding it to the NMR sample. The p53 peptide was titrated to a final concentration of 4.8−5.3 mM into S100B($\beta\beta$)−Ca^{2+} samples.

The unlabeled S100B($\beta\beta$) sample was used to collect 2D NOESY (*39*) and 2D TOCSY (*40*). The uniformly ^{15}N-labeled S100B($\beta\beta$) sample was used to collect a two-dimensional ^{1}H−^{15}N fast HSQC (*41*), a 3D ^{15}N-edited NOESY−HSQC (*42*) with a 100 ms mixing time, a 3D ^{15}N-edited clean-HOHAHA-HSQC (*40*, *43*) with a 70 ms spin-lock time using a 10 kHz rf field strength and a DIPSI-2rc mixing sequence (*44*), and a 3D ^{15}N,^{15}N-edited HMQC−NOESY−HSQC (*45*) with a 150 ms mixing time (Table 1). The ^{13}C,^{15}N-labeled S100B($\beta\beta$) sample was used to collect the 3D HNCACB (*46*), 3D CBCA(CO)NH (*47*), HCCH-TOCSY (*48*, *49*), 3D ^{13}C-edited HMQC−NOESY (*50*), the sensitivity-enhanced 4D ^{13}C,^{15}N-edited NOESY−HSQC (*51*) with a 100 ms mixing time, and 4D ^{13}C,^{13}C-edited NOESY HSQC (*52*). In all of the ^{15}N-edited experiments, the fast-HSQC detection scheme was incorporated into the sequence to avoid water saturation (*41*). Furthermore, pulsed field gradients were used as needed to purge undesired magnetization (*53*).

Metal and p53 Peptide Binding to S100B($\beta\beta$). The concentration of free Mn^{2+} in a mixture of free and bound Mn^{2+} was determined by electron paramagnetic resonance (*54*) using a Varian E-4 EPR spectrometer with the temperature maintained at 22 °C. These data were supplemented by studies of bound Mn^{2+} under the same conditions by measuring the longitudinal relaxation rates of water protons at 24.3 MHz with a 180°−τ−90° pulse sequence using a Seimco pulsed NMR spectrometer as described previously (*55*, *56*). The observed enhancement of the water proton relaxation rate is defined as $\epsilon^* = (1/T_{1P}^*)/(1/T_{1P})$ where $1/T_{1P}$ is the paramagnetic contribution to the longitudinal relaxation rate in the presence (*) and absence (no symbol) of S100B($\beta\beta$) (*56*). The NMR and EPR data were analyzed to determine the stoichiometry (n) of Mn^{2+} bound to S100B($\beta\beta$), the dissociation constant (K_D), and the enhancement factor (ϵ_b) of the S100B($\beta\beta$)−Mn^{2+} complex as previously

described (*56*−*62*). In addition, the binding of Mn^{2+} to S100B($\beta\beta$) in the presence of the p53 peptide ($^{Mn}K_2$) was monitored by EPR and by changes in $1/T_{1P}$* of water protons, providing independent measurements of the dissociation constants of Mn^{2+} from the S100B($\beta\beta$)−Mn^{2+}−p53 peptide complex. The titration of the S100B($\beta\beta$)−Mn^{2+} complex with p53 peptide was monitored by changes in the $1/T_{1P}$ of water protons and the observed enhancement factor (ϵ*); also, at least 30 min passed prior to each peptide addition. A dissociation constant ($^{Mn}K_3$) of the p53 peptide from the S100B($\beta\beta$)−Mn^{2+}−p53 peptide complex was first analyzed using a noncooperative binding model to find the dissociation constant ($^{Mn}K_3$) and enhancement factors (ϵ_T) as previously described (*56*, *60*, *63*). However, data from the $^{Mn}K_3$ titration were fit much better by a cooperative binding model using the Hill equation and Hill coefficient of $n_H = 2.3 \pm 0.2$.[2] Dissociation constants of Ca^{2+}, Zn^{2+}, and La^{3+} from the tight site of S100B($\beta\beta$) in the absence and in the presence of p53 peptide were obtained by competition experiments in which the corresponding Mn^{2+} complex was titrated with metal, monitoring the displacement of Mn^{2+} by changes in the enhancement (ϵ*) of $1/T_{1P}$* and independently by the appearance of free Mn^{2+} in the EPR spectrum. The concentrations of $CaCl_2$, $ZnCl_2$, and $LaCl_3$ used in these studies were determined by atomic absorption spectroscopy (Quantitative Technologies Inc., Whitehouse, NJ), and the $MnCl_2$ concentration was determined by comparing the $1/T_{1P}$ of stock solutions to that of a Mn^{2+} sample of known concentration as previously described (*56*).

RESULTS AND DISCUSSION

Previously, Baudier and co-workers showed that full-length p53 is a substrate for PKC in vivo and in vitro (*19*). They also showed that S100B($\beta\beta$) interacts with p53 in a Ca^{2+}-dependent manner to inhibit phosphorylation and tetramer formation (*19*). Since phosphorylation at the C-terminus of p53 is known to affect transcription and p53 tetramer formation (*27*, *28*), we examined the interaction of S100B($\beta\beta$) with a peptide derived from the C-terminal regulatory domain of p53 (residues 367−388) using fluorescence and magnetic resonance techniques.

Binding of the p53 Peptide to S100B($\beta\beta$). (A) Fluorescence Spectroscopy. A mutant p53 peptide was prepared in which we substituted the phenylalanine at position 385 with a tryptophan (F385W p53 peptide) since no change could be detected in the fluorescence signal from the single tyrosine residue (Y17) in S100B($\beta\beta$) during titrations with wild-type p53 peptide. Figure 1A (inset) illustrates a typical titration in which S100B($\beta\beta$) was added to a solution containing the F385W p53 peptide and an increase in fluorescence intensity was measured. The dissociation constant was determined ($^{p53F385W-Ca}K_3 = 6.4 \pm 1.1$ μM) for this titration using a noncooperative binding model with a single peptide bound per S100β subunit. In the absence of Ca^{2+}, no change in fluorescence was observed upon the addition of S100B($\beta\beta$).

In subsequent titrations with wild-type peptide, the F385W p53 peptide was displaced and monitored by a change in fluorescence intensity (Figure 1A). A cooperative binding model was used (Hill coefficient $n_H = 3.2 \pm 0.8$) to fit the competition data for the wild-type peptide.[2] The Hill coefficient suggests that positive cooperativity occurs for peptide binding; however, a slow kinetic step at low peptide concentrations cannot be completely ruled out. Thus, an apparent dissociation constant was determined (Figure 1A), and the upper limit for the dissociation constant ($^{Ca}K_3 \leq 23.5 \pm 6.6$ μM) was calculated as described under Experimental Procedures. Furthermore, the dissociation of the p53 peptide from the Ca^{2+} complex ($^{Ca}K_3 \leq 23.5 \pm 6.6$ μM) readily explains the concentration of S100B($\beta\beta$) required for 50% inhibition of PKC-dependent phosphorylation determined previously in kinetic studies ($^{S100B}IC_{50} = 10 \pm 7$ μM) (*26*).

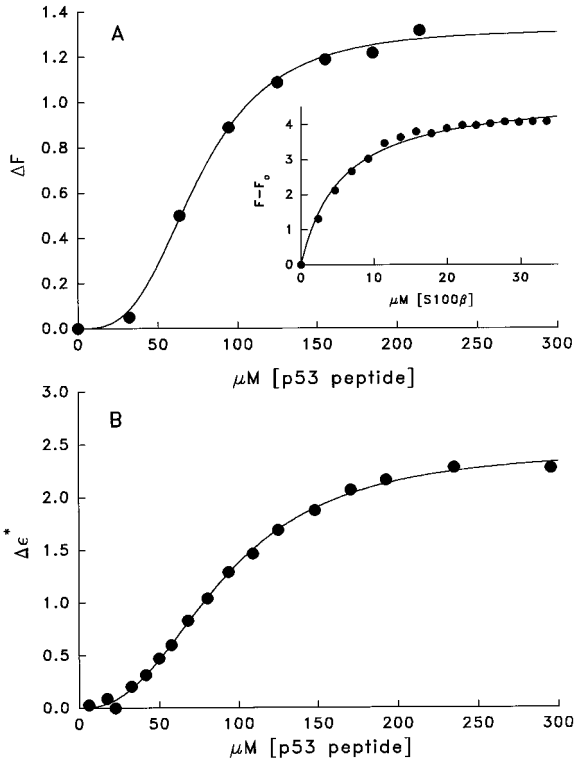

FIGURE 1: Measurement of p53 peptide binding to the S100B($\beta\beta$)−Ca^{2+} and S100B($\beta\beta$)−Mn^{2+} complexes. (A) Fluorescence titration monitoring the displacement of the F385W p53 peptide from S100B($\beta\beta$) upon binding of the wild-type p53 peptide. The solution contained 20 μM S100β. (A, inset) Fluorescence titration of p53F385W peptide (14 μM) with S100B. The increase of emission from the F385W p53 peptide at $\lambda = 338$ nm is plotted as a function of S100β concentration. In these titrations, the solutions contained 25 mM Tris-HCl, 6 mM NaCl, 6 mM $CaCl_2$, 2 mM DTT, pH 7.6, 22 °C. (B) Titration of the S100B($\beta\beta$)−Mn^{2+} complex with p53 peptide is monitored by measuring the changes in the Mn^{2+}-induced enhancement (ϵ*) of water protons, $1/T_{1P}$. The solution contained 50 mM Tris-HCl, 130 μM S100β, 47.7 μM Mn^{2+}, pH 7.5, at 22 °C. To avoid dilution effects, the p53 peptide was added from a concentrated stock solution that contained all of the other components of the titration at the same final concentration.

The blue shift observed in the fluorescence emission maxima (from $\lambda = 350$ nm to $\lambda = 338$ nm) of the F385W p53 peptide upon addition of the S100B($\beta\beta$)−Ca^{2+} complex indicates that the tryptophan residue of the peptide binds to a hydrophobic domain present in S100B($\beta\beta$)−Ca^{2+}. Second, the affinity for wild-type p53 peptide may be as much as 4-fold lower than the mutant peptide ($^{p53F385W-Ca}K_3 = 6.4 \pm 1.1$ μM versus $^{Ca}K_3 \leq 23.5 \pm 6.6$ μM), most likely because phenylalanine is not as large of a hydrophobic residue (by 1.4-fold) as tryptophan. These results together support the hypothesis (*6*−*8*) that a hydrophobic patch is exposed on the S100B($\beta\beta$)−Ca^{2+} complex which is at least partially responsible for binding target proteins.

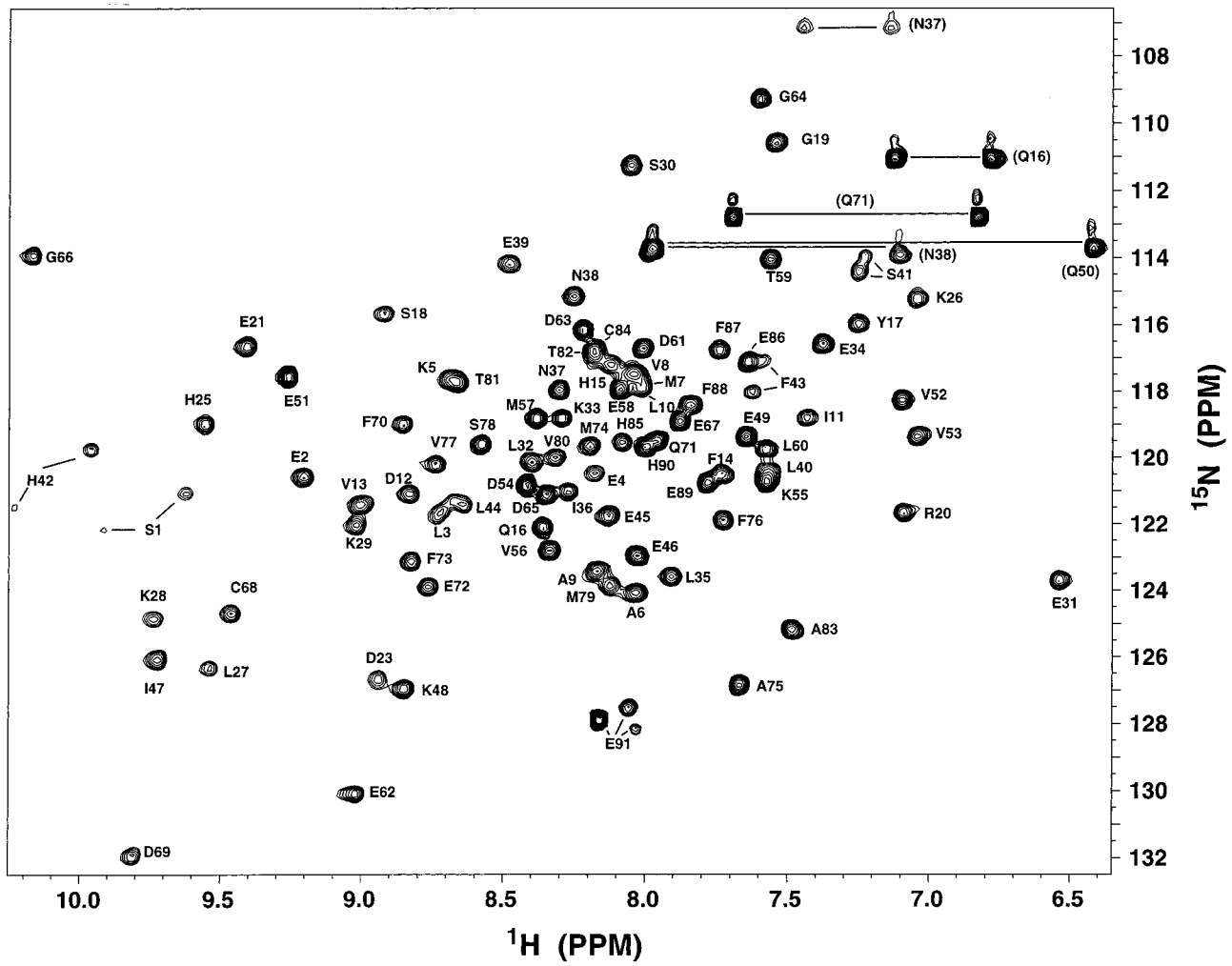

FIGURE 2: 2D ^{1}H−^{15}N fast HSQC spectra of S100B($\beta\beta$) in the S100B($\beta\beta$)−Ca^{2+}−p53 complex. ^{1}H−^{15}N fast HSQC spectrum of S100B($\beta\beta$) in the S100($\beta\beta$)−Ca^{2+}−p53 complex showing all of the ^{1}H−^{15}N correlations together with their sequential assignments. The correlations connected by horizontal lines correspond to glutamine and asparagine side-chain NH_2 groups. The assignments with extra correlations (S1, S41, H42, and F43) are due to the presence or absence of a formyl group at the amino terminus as previously described (*1*). The sample conditions are 3.2 mM S100β, 0.34 mM NaN_3, 10 mM Tris-d_{11}, 17 mM NaCl, 5 mM DTT, 0.1 mM EDTA, 10% D_2O, 6.3 mM $CaCl_2$, 5.1 mM p53 peptide, 37 °C.

(B) NMR Spectroscopy. Titrations of S100B($\beta\beta$) with p53 peptide were monitored by NMR spectroscopy in order to determine which residues of S100B($\beta\beta$) are most affected by p53 peptide binding. In the presence of Ca^{2+}, a large number of resonances in the HSQC spectrum of S100B($\beta\beta$) shifted significantly (>0.2 ppm) upon the addition of p53 peptide (Figures 2, 3). Whereas no changes in chemical shift or line shape were observed when the p53 peptide was titrated into S100B($\beta\beta$) in the absence of Ca^{2+} (data not shown). These data again confirm the Ca^{2+} dependence of the p53 peptide interaction with S100B($\beta\beta$). During p53 peptide titration, most of the correlations shifted with no peak doubling,[3] the ^{15}N and ^1H_N line widths broadened by about 1−3 Hz, and the ^{15}N−^1H_N correlations stopped shifting when the ratio of peptide to S100B($\beta\beta$)−Ca^{2+} was approximately 1.6 to 1. Together these data suggest that one p53 peptide binds each subunit of the S100B($\beta\beta$) dimer, and that binding of the peptide occurs in a symmetric manner.

At the end of p53 peptide titration, the resonance assignments of S100B($\beta\beta$) were verified using standard methods (*64*). Thus, the identification of each spin system was determined using a ^{15}N-edited clean-HOHAHA-HSQC, 3D HCCH-TOCSY, 2D NOESY, 2D TOCSY, and 4D ^{13}C,^{13}C-edited NOESY, and sequence-specific assignments were made using characteristic αN(i,i+1), NN(i,i+1), and NN(i,i+2) NOE correlations in 3D ^{15}N-edited NOESY−HSQC, 3D ^{15}N,^{15}N-edited HMQC−NOESY−HSQC, and 4D ^{13}C,^{15}N-edited NOESY−HSQC spectra as previously described (*65*) (data not shown). Furthermore, 3D data from the HNCACB and CBCA(CO)NH experiments were collected in order to unambiguously complete the sequential resonance assignments as previously described for apo-S100B($\beta\beta$) (*12*, *64*). The ^{1}H−^{15}N HSQC spectrum of S100B($\beta\beta$) in the S100B($\beta\beta$)−Ca^{2+}−p53 peptide complex is shown in Figure 2, illustrating the assignments for the backbone amide correlations.[4]

The differences in ^1H_N and ^{15}N chemical shifts between the S100B($\beta\beta$)−Ca^{2+} and the S100B($\beta\beta$)−Ca^{2+}−p53 pep-

[3] Residue S41 is the one exception where peak doubling occurred as a result of adding p53 peptide (Figures 2 and 3B). In this case, however, the peak doubling is most likely the result of S41 approaching the N-terminus where there is a mixture of formylated and free N-terminal methionine (M0), as previously described (*1*). Residues S1, H42, and F43 are doubled both in the presence and in the absence of p53 peptide most likely because of their proximity to the N-terminus (*1*).

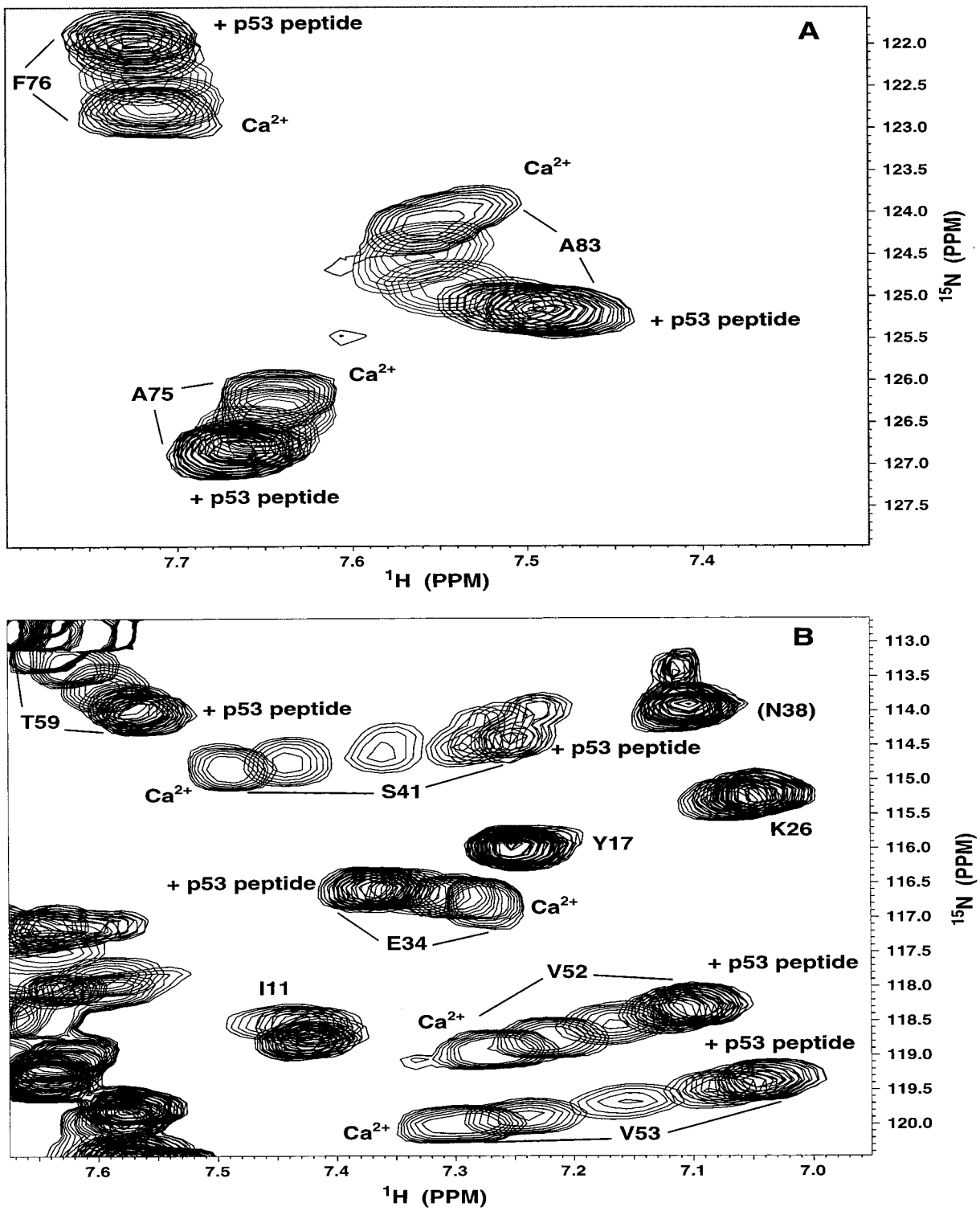

FIGURE 3: Regions of the $^1H-^{15}N$ fast HSQC spectrum illustrating changes in the chemical shift upon the addition of p53 peptide to Ca^{2+}-bound S100B($\beta\beta$). The starting point in the titration has no p53 peptide and is labeled Ca^{2+}, and the final point in the titration has 5.1 mM p53 peptide and is labeled + p53 peptide. (A) Resonances in the C-terminal loop (A83) and helix 4 (A75, F76) that change upon addition of p53 peptide to the S100B($\beta\beta$)$-Ca^{2+}$ complex. (B) Region of $^1H-^{15}N$ fast HSQC spectrum illustrating changes in chemical shift for resonances in helix 2 (E34), the hinge region (S41), and helix 3 (V52, V53, T59). The correlation for N38 in parentheses corresponds to the asparagine side-chain NH_2 group.

tide complexes are plotted as a function of amino acid residue number (Figure 4). While changes in chemical shift are observed for most residues in S100B($\beta\beta$), residues in helix 1 (L3), the hinge region (S41, L44, E45, E46, I47), the normal EF-hand (E62), helix 3 (V52, V53, V56, T59), helix 4 (S78, M79, T81, T82), and the C-terminal loop (A83, C84, H85, E86, F87, F88) are most affected (>0.2 ppm ^1H and/or >1.0 ppm ^{15}N). These residues also show different NOE correlations than that of the S100B($\beta\beta$)$-Ca^{2+}$ complex (*66*) (Figure 5). Changes in chemical shift and NOE correlations for these residues are likely the result of a direct interaction of the peptide with the S100B($\beta\beta$)$-Ca^{2+}$ complex; however, the possibility of the p53 peptide inducing structural changes at or nearby these residues upon binding cannot be ruled

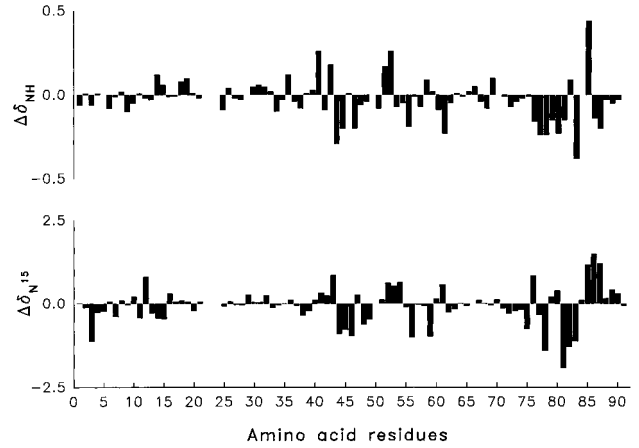

FIGURE 4: Plot of ^1H_N and ^{15}N chemical shift changes for each amino acid residue after a titration of the S100B($\beta\beta$)−Ca^{2+} complex with the p53 peptide. Conditions are described in Figure 2.

FIGURE 5: Ribbon diagram of dimeric Ca^{2+}-bound S100B($\beta\beta$) (*66*). The darkest shaded regions illustrate the residues which change in chemical shift (^1H > 0.2 ppm and ^{15}N > 1.0 ppm) and which have new NOE correlations upon the addition of the p53 peptide. The two subunits of Ca^{2+}-bound S100B($\beta\beta$) are also shaded differently.

out. It should also be noted that out of these 21 residues, 15 are hydrophobic and could be part of the hydrophobic patch that interacts with a hydrophobic region on the wild-type p53 peptide (L383, M384, F385, T387) and the F385W mutant. In addition, three glutamate residues located in the hinge and C-terminal loop of S100B($\beta\beta$) (E45, E46, and E86) could be candidates for interacting with the basic residues of the p53 peptide (H368, K370, K372, K373).

[4] The ^1H, ^{13}C, and ^{15}N chemical shift values for S100B($\beta\beta$) in the S100B($\beta\beta$)−Ca^{2+} and S100B($\beta\beta$)−Ca^{2+}−p53 peptide complexes have been deposited in the BioMagResBank chemical shift data bank located at the University of Wisconsin at Madison (4099). They will also be described in more detail in separate publications regarding the structure of each complex.

Table 2: Dissociation of Metal Ions from S100B($\beta\beta$)−Metal and S100B($\beta\beta$)−Metal−p53 Peptide Complexes[a]

metal ions	K_D (μM)[b]	K_2 (μM)[c]	K_3 (μM)[d]
Ca^{2+} [e]	55.9 ± 9.0 (2)	20.4 ± 3.1 (5)	≤ 23.5 ± 6.6 (3)
La^{3+} [e]	13.7 ± 2.8 (3)	3.4 ± 0.5 (2)	−
Zn^{2+}	6.9 ± 1.8 (3)	5.3 ± 0.8 (3)	−
Mn^{2+} [f]	71.4 ± 12.0 (2)	27.0 ± 4.0 (2)	≤ 94.7 ± 20.4 (4)

[a] The number of experiments (n) is shown in parentheses. [b] Dissociation constant of metals from the tight site of S100B($\beta\beta$). [c] Dissociation constant of metals from the tight site of S100B($\beta\beta$) in the presence of the p53 peptide. [d] Dissociation constant of p53 peptide from S100B($\beta\beta$) in the presence of metal. The F385W mutant peptide was found to bind Ca^{2+}-bound S100B($\beta\beta$) with a $K_3 = 6.4 \pm 1.1$ μM. [e] Total metal ion was corrected for minimal binding to the weak site (pseudo-EF-hand); in no cases did this correction exceed 10% of the total metal ion concentration. [f] The enhancement factor in the K_D titration using PRR was $\epsilon_b = 7.0 \pm 1.1$, and the enhancement factor in the K_2 and K_3 titration using PRR was $\epsilon_T = 3.2 \pm 1.1$.

Of the 21 resonances in S100B($\beta\beta$) that change appreciably, 11 of them are grouped in the hinge region (S41, L44, E45, E46, I47) and the C-terminus (A83, C84, H85, E86, F87, F88). This is particularly interesting because the hinge region and the C-terminal loop are proximal in the structure of apo-S100B($\beta\beta$) (*10*), and they are implicated in binding target proteins for a number of S100 proteins (*7*). For example, the hinge region of another S100 protein, CP-10, was found to exhibit chemotactic activity similar to that of full-length protein (*67*). Furthermore, mutation of residues in the C-terminus of p11 was found to abolish annexin I binding (*68*). Chemical modification and mutagenesis of C84 in S100B($\beta\beta$) were found to decrease binding to τ-protein (*69*) and aldolase (*70*), respectively, and further implicate the C-terminus as an important region of S100B($\beta\beta$) for target protein binding. Finally, the specificity of target protein binding is attributed to the hinge and C-terminal loops since they are the least conserved regions of S100 proteins (*7*). Thus, the change in chemical shift observed for residues in the hinge region and the C-terminal loop are most likely the result of a direct interaction between Ca^{2+}-loaded S100B($\beta\beta$) and the p53 peptide.

Effects of p53 Peptide on S100B($\beta\beta$) Metal Ion Binding. Binding studies with Mn^{2+} were completed since it is a good probe of both Ca^{2+} and Zn^{2+} binding sites (*71*). The dissociation of the p53 peptide from the S100B($\beta\beta$)−Mn^{2+}−p53 peptide complex was measured first to verify that the p53 peptide could bind S100B($\beta\beta$) in the presence of Mn^{2+}. A solution containing S100B($\beta\beta$) and Mn^{2+} was titrated with the p53 peptide, and changes in the enhancement (ϵ*) of $1/T_{1P}$ of water protons were monitored (*56*). A typical titration curve is shown in Figure 1B in which the change in the enhancement of proton relaxation ($\Delta\epsilon$*) is plotted as a function of p53 peptide concentration. The data were best fit using the Hill equation with a dissociation constant of $^{Mn}K_3 \leq 94.7 \pm 20.4$ μM ($n_H = 2.3 \pm 0.2$; Table 2).[2] Although the p53 peptide binds S100B($\beta\beta$) in the presence of Mn^{2+} ($^{Mn}K_3 \leq 94.7 \pm 20.4$ μM), its affinity is lower than in the presence of Ca^{2+} ($^{Ca}K_3 \leq 23.5 \pm 6.6$ μM), suggesting a preference for peptide binding when Ca^{2+} is present.

A S100B($\beta\beta$)−Mn^{2+} complex was studied by titration of the protein with $MnCl_2$ since free Mn^{2+} can be measured

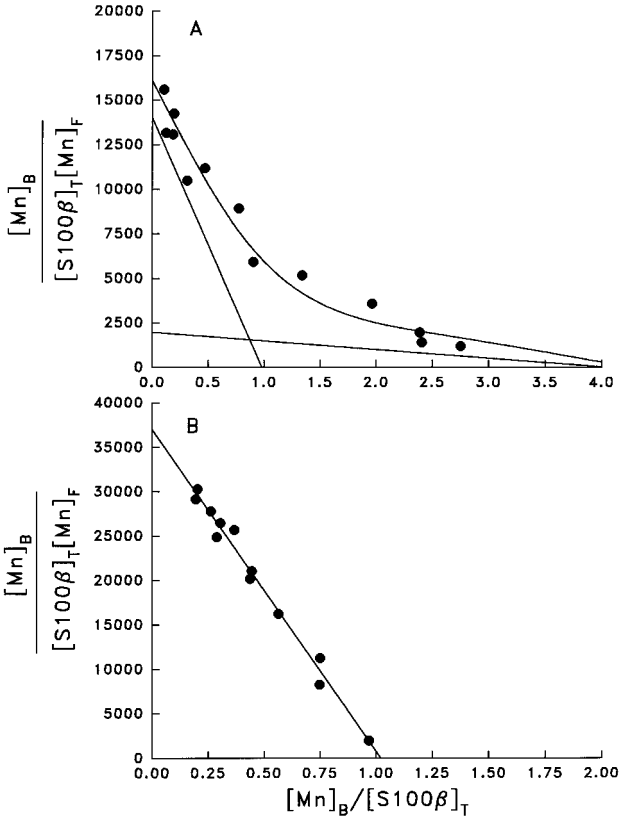

FIGURE 6: Scatchard plots of Mn^{2+} binding to S100B($\beta\beta$) in the absence or presence of the p53 peptide. (A) In the absence of p53 peptide, two solid lines representing the tight and weak Mn^{2+} binding sites are shown together with a curve fitting the data as previously described (*78*). (B) In the presence of the p53 peptide (150 μM), the data were best fit to a straight line, and data representing the weak Mn^{2+} binding site(s) are not shown. In both cases, free Mn^{2+} was measured by EPR at 22 °C, and the solutions contained 65 μM S100β, 50 mM Tris-HCl, pH 7.6.

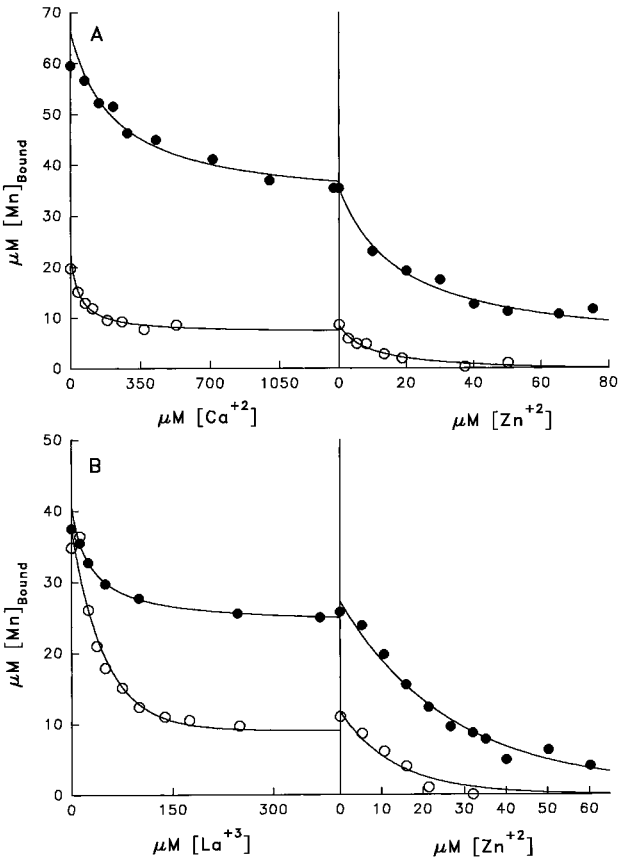

FIGURE 7: Displacement of bound Mn^{2+} by Ca^{2+} or La^{3+}, and then by Zn^{2+} from S100B($\beta\beta$) as detected by EPR. (A) Displacement of Mn^{2+} from S100β by Ca^{2+} and then by Zn^{2+} in the absence (filled circles) and presence (open circles) of p53 peptide. The solution in the absence of peptide (filled circles) contains 62.1 μM S100β and 187.1 μM Mn^{2+}, and the solution in the presence of 150 μM p53 peptide (open circles) contains 64.8 μM S100β and 28.6 μM Mn^{2+}. (B) Displacement of Mn^{2+} by La^{3+} and then by Zn^{2+} in the absence (filled circles) and presence (open circles) of p53 peptide is also shown. The solution in the absence of peptide (filled circles) contains 64.8 μM S100β and 70.2 μM Mn^{2+}, and the solution in the presence of 150 μM p53 peptide (open circles) contains 62.1 μM S100β and 73.2 μM Mn^{2+}. All four solutions contained 50 mM Tris-HCl, pH 7.5. To avoid dilution effects, Ca^{2+}, La^{3+}, and Zn^{2+} were added from concentrated stock solutions that contained all of the other components of the titration at the same final concentration. In each case, the data are shown together with best-fit K_{app} curves. The corresponding dissociation constants were calculated using competition equations as described previously (*59*, *62*).

directly using EPR. The enhancement (ϵ*) of $1/T_{1P}$ of water protons was also determined by low-field pulsed NMR as a function of Mn^{2+} bound to S100B($\beta\beta$). The values for free and bound Mn^{2+} were analyzed with a Scatchard plot and compared to similar titrations performed in the presence of the p53 peptide (Figure 6; Table 2). Interestingly, the presence of the p53 peptide increased the affinity of the single tight Mn^{2+} site by 2.6-fold ($^{Mn}K_D = 71.4$ μM versus $^{Mn}K_2 =$ 27.0 μM; Table 2). In addition, approximately four weak Mn^{2+} sites ($K_D \approx 2$ mM) were also detected. Control experiments indicated that peptide alone did not bind Mn^{2+} ($K_1 > 5$ mM).

Displacement of Mn^{2+} from the S100B($\beta\beta$)−Mn^{2+} and S100B($\beta\beta$)−Mn^{2+}−p53 peptide complexes by Ca^{2+}, Zn^{2+}, and La^{3+} was done to obtain dissociation constants for each of these metal ions. Titrations of Ca^{2+}, Zn^{2+}, or La^{3+} were monitored by measuring the appearance of free Mn^{2+} by EPR (Figure 7) and by changes in enhancement (ϵ*) using NMR. Figure 7A illustrates that Ca^{2+} is able to displace Mn^{2+} from its tight site in the absence ($^{Ca}K_D = 55.9$ μM) or presence ($^{Ca}K_2 = 20.4$ μM) of the p53 peptide, and as for Mn^{2+}, the presence of peptide enhanced the affinity of Ca^{2+} by ≈3-fold. Likewise, the peptide increases the affinity of La^{3+} by 4-fold when binding in the absence and presence of peptide are compared (Table 2; Figure 7B). It is clear that Mn^{2+} is displaced from the normal EF-hand in S100B($\beta\beta$) (residues 61−72) since the K_D from these competition studies ($^{Ca}K_D = 55.9 \pm 9.0$ μM) is similar to that observed previously for the tight Ca^{2+}-binding site using equilibrium dialysis ($^{Ca}K_D = 35 \pm 15$ μM) (*15*). However, increasing amounts of Ca^{2+} (>2 mM) were not sufficient to displace any of the Mn^{2+} that remains bound to S100B($\beta\beta$) (data not shown), indicating that the pseudo-EF-hand (residues 18−31) does not bind Mn^{2+} under these conditions. However, low concentrations of Zn^{2+} readily displaced the remaining Mn^{2+} both in the presence and in the absence of p53 peptide ($^{Ca-Zn}K_D = 6.9 \pm 1.8$ μM; $^{Ca-Zn}K_2 = 5.3 \pm$ 0.8 μM), respectively (Figure 7A; Table 2). Thus, the presence of peptide did not affect the affinity of Ca^{2+}-loaded S100B($\beta\beta$) for binding Zn^{2+}. Moreover, in the absence of Ca^{2+} or La^{3+}, Zn^{2+} could displace all of the Mn^{2+} present in the tight and weak sites of both complexes (data not shown).

The binding of metal ions to S100B($\beta\beta$) is known to induce a large conformational change [for review, see (*6*−*8*, *66*)]. The solution structure of rat apo-S100B($\beta\beta$) (*10*) illustrates that the interhelical angle in the classical EF-hand (helixes 3:4; 218 ± 3°) is quite different from that found in apo-calbindin D_{9K} (helix 3:4; 118 ± 8°) and that a very large change in the interhelical angle between helixes 3 and 4 (−113 ± 24°) must occur upon binding Ca^{2+} in order for this EF-hand to assume a similar orientation as that found in Ca^{2+}-loaded calmodulin or calbindin D_{9K} (*10*, *16*). The geometry of the EF-hand coordination is most likely improved in the presence of the p53 peptide, perhaps by stabilizing the position of helix 3, since metal ion binding studies show that S100B($\beta\beta$) has a higher affinity (3−4-fold) for Ca^{2+}, La^{3+}, and Mn^{2+} in the presence of peptide than in its absence, whereas the affinity for Zn^{2+}, which binds at a different site, was not affected by the peptide target. Also, changes in chemical shift for several residues (V52, V53, V56, T59) in helix 3 upon addition of p53 peptide further support the notion that peptide binding reorients this helix and improves Ca^{2+} coordination (Figures 2 and 3).

An alternate mechanism for the increased metal ion affinity is that the peptide itself provides a ligand directly to Ca^{2+}. This latter hypothesis is unlikely, since lanthanide luminescence spectroscopy experiments indicate that the coordination sphere of Ca^{2+} bound to S100B($\beta\beta$) in the absence of peptide is fully occupied as found for the high-affinity Ca^{2+}-binding domains (1 and 2) in calmodulin (*16*). Furthermore, only a few changes in chemical shift were observed for residues in the second EF-hand (residues 61−72) upon the addition of p53 peptide (Figure 4) which is evidence that the peptide does not approach these residues, but rather it has an indirect effect on Ca^{2+} binding.

Implications for p53 Phosphorylation. Short synthetic peptides are widely used to study the site of phosphorylation for a number of protein kinases since they often contain the entire kinase recognition motif and give kinetic properties similar to those of the full-length substrate (*72*). Furthermore, a series of studies completed by Blackshear and coworkers found that the behavior of peptides from the phosphorylation site/calmodulin-binding domain (termed PSCBD peptides) are excellent models for studying PKC-dependent phosphorylation kinetics and calmodulin binding (*73*−*76*). In our studies, the phosphorylation site/S100B-binding domain of p53 (residues 367−388) was found to be a good substrate for the catalytic domain of PKC (K_m = 1.8 ± 0.4 μM; V_{max} = 1.6 ± 0.2 μmol min^{-1} mg^{-1}), and its PKC-dependent phosphorylation was inhibited by S100B($\beta\beta$) in a Ca^{2+}-dependent manner (*25*, *26*). Furthermore, the Ca^{2+}-dependent interaction of S100B($\beta\beta$) and the p53 peptide ($^{Ca}K_3 \leq 23.5 \pm 6.6$ μM) observed here can explain the concentration of S100B($\beta\beta$) required for 50% inhibition of PKC-dependent phosphorylation of the p53 peptide ($^{S100B}IC_{50}$ = 10 ± 7 μM). Therefore, we suggest that the p53 peptide is a good model for studying the Ca^{2+}-dependent interaction of S100B($\beta\beta$) with the PKC phosphorylation domain located in the C-terminus of p53.

The ability of S100B($\beta\beta$) to inhibit the PKC-dependent phosphorylation of the p53 peptide can be explained by its binding to the p53 peptide substrate rather than by interactions with the enzyme. Furthermore, at least the tight Ca^{2+} site of each S100β subunit must be saturated in order to completely inhibit PKC-dependent phosphorylation as determined by comparing the Ca^{2+}-dependent inhibition constant determined previously ($^{Ca}IC_{50}$ = 29.3 ± 17.6 μM) (*26*) to the dissociation constant of Ca^{2+} from the tight site of S100β with the p53 peptide present ($^{Ca}K_2$ = 20.4 ± 3.1 μM) (Table 2). While a direct interaction between p53 and S100B($\beta\beta$) has not yet been demonstrated in vivo, the in vitro interaction between the C-terminal regulatory domain of p53 and S100B($\beta\beta$) illustrated in this paper may provide important clues for examining how S100B($\beta\beta$) is involved in cell-cycle processes at the G_0-G_1/S transition. In addition, perhaps a general mechanism for regulating signal transduction is emerging since another Ca^{2+}-binding protein, calmodulin, is known to inhibit the PKC-dependent phosphorylation of MARCKS and MARCKS-related proteins (MRPs) by directly binding the protein substrate (*73*, *77*). Thus, S100 proteins and calmodulin may provide a preemptive control mechanism in signal transduction which is, in some sense, opposite to the control mechanism provided by protein phosphatases which react after a signal is transduced.

ACKNOWLEDGMENT

We are grateful to Dr. A. Mildvan for use of the proton relaxation NMR and EPR instruments and to Dr. Richard Thompson for help with the fluorescence spectroscopy. We are also grateful to Drs. Linda Van Eldik and Enrico Bucci for helpful discussions

REFERENCES

1. Smith, S. P., Barber, K. R., and Shaw, G. S. (1997) *Protein Sci. 6*, 1110−1113.
2. Moore, B. (1965) *Biochem. Biophys. Res. Commun. 19*, 739−744.
3. Takashi, M., Sakata, T., Nakano, Y., Yamada, Y., Miyake, K., and Kato, K. (1994) *Urol. Res. 22*, 251−255.
4. Suzushima, H., Hattori, T., and Takatasuki, K. (1994) *Leuk. Lymph. 13*, 257−262.
5. Donato, R. (1991) *Cell Calcium 12*, 713−726.
6. Zimmer, D. B., Cornwall, E. H., Landar, A., and Song, W. (1995) *Brain Res. Bull. 37*, 417−429.
7. Kligman, D., and Hilt, D. (1988) *Trends Biochem. Sci. 13*, 437−443.
8. Schafer, B. W., and Heizmann, C. W. (1996) *Trends Biochem. Sci. 21*, 134−140.
9. Drohat, A. C., Nenortas, E., Beckett, D., and Weber, D. J. (1997) *Protein Sci. 6*, 1577−1582.
10. Drohat, A. C., Amburgey, J. C., Abildgaard, F., Starich, M. R., Baldisseri, D., and Weber, D. J. (1996) *Biochemistry 35*, 11577−11588.
11. Kilby, P. M., Van Eldik, L. J., and Roberts, G. C. K. (1996) *Structure 4*, 1041−1052.
12. Amburgey, J. C., Abildgaard, F., Starich, M. R., Shah, S., Hilt, D. C., and Weber, D. J. (1995) *J. Biomol. NMR 6*, 171−179.
13. Kretsinger, R. H. (1980) *CRC Crit. Rev. Biochem. 8*, 119−174.
14. Strynadka, N. C. J., and James, M. N. G. (1989) *Annu. Rev. Biochem. 58*, 951−998.
15. Baudier, J., Glasser, N., and Gerard, D. (1986) *J. Biol. Chem. 261*, 8192−8203.
16. Chaudhuri, D., Horrocks, W. W., Amburgey, J. C., and Weber, D. J. (1997) *Biochemistry 36*, 9674−9680.
17. Bianchi, R., Giambanco, I., and Donato, R. (1993) *J. Biol. Chem. 268*, 12669−12674.
18. Bianchi, R., Verzini, M., Garbuglia, M., Giambanco, I., and Donato, R. (1994) *Biochim. Biophys. Acta 1223*, 354−360.
19. Baudier, J., Delphin, C., Grundwald, D., Khochbin, S., and Lawrence, J. J. (1992) *Proc. Natl. Acad. Sci. U.S.A. 89*, 11627−11631.

20. Baudier, J., Mochly-Rosen, D., Newton, A., Lee, S.-H., Koshland, D. E., and Cole, R. D. (1987) *Biochemistry 26*, 2886−2893.
21. Lin, L.-H., Van Eldik, L. J., Osheroff, N., and Nordon, J. J. (1994) *Mol. Brain Res. 25*, 297−304.
22. Sheu, F.-S., Azmitia, E. C., Marshak, D. R., Parker, P. K., and Routtenberg, A. (1994) *Mol. Brain Res. 21*, 62−66.
23. Patel, J., Marangos, P. J., Heydorn, W. E., Chang, G., Verma, A., and Jacobowitz, D. (1983) *J. Neurochem. 41*, 1040−1045.
24. Albert, K. A., Wu, W. C.-S., Nairn, A. C., and Greengard, P. (1984) *Proc. Natl. Acad. Sci. U.S.A. 81*, 3622−3625.
25. Wilder, P. T., and Weber, D. J. (1996) *Biophys. J. 70*, A62.
26. Wilder, P. T., Rustandi, R. R., Drohat, A. C., and Weber, D. J. (1998) *Protein Sci.* (in press).
27. Sakaguchi, K., Sakamoto, H., Lewis, M. S., Anderson, C. W., Erickson, J. W., Appella, E., and Xie, D. (1997) *Biochemistry 36*, 10117−10124.
28. Takenaka, I., Morin, F., Seizinger, B. R., and Kley, N. (1995) *J. Biol. Chem. 270*, 5405−5411.
29. Hupp, T. R., Sparks, A., and Lane, D. P. (1995) *Cell 83*, 237−245.
30. Fasman, G. D. (1990) *CRC Practical Handbook of Biochemistry and Molecular Biology*, CRC Press, Boca Raton, FL.
31. Marion, D., Ikura, M., Tschudin, R., and Bax, A. (1989) *J. Magn. Reson. 85*, 393−399.
32. Bax, A., Ikura, M., Kay, L. E., and Zhu, G. (1991) *J. Magn. Reson. 91*, 174−178.
33. Delaglio, F., Grzesiek, S., Vuister, G. W., Zhu, G., Pfeifer, J., and Bax, A. (1995) *J. Biomol. NMR 6*, 277−293.
34. Zhu, G., and Bax, A. (1992) *J. Magn. Reson. 98*, 192−199.
35. Zhu, G., and Bax, A. (1990) *J. Magn. Reson. 90*, 405−410.
36. Live, D. H., Davis, D. G., Agosta, W. C., and Cowburn, D. (1984) *J. Am. Chem. Soc. 106*, 1939−1941.
37. Spera, S., and Bax, A. (1991) *J. Am. Chem. Soc. 113*, 5490−5492.
38. Edison, A. S., Abilgaard, F., Westler, W. M., Mooberry, E. S., and Markley, J. L. (1994) *Methods Enzymol. 239*, 3−79.
39. Jeener, J., Meier, B. H., Bachmann, P., and Ernst, R. R. (1979) *J. Chem. Phys. 71*, 4546−4553.
40. Bax, A., and Davis, D. G. (1985) *J. Magn. Reson. 65*, 355−360.
41. Mori, S., Abeygunawardana, C., Johnson, M. O., and Van Zijl, P. C. M. (1995) *J. Magn.* Reson. *108*, 94−98.
42. Kay, L. E., Marion, D., and Bax, A. (1989) *J. Magn. Reson. 84*, 72−84.
43. Marion, D., Driscoll, P. C., Kay, C. M., Wingfield, P. T., Bax, A., Gronenborn, A. M., and Clore, G. M. (1989) *Biochemistry 28*, 6150−6156.
44. Cavanagh, J., and Rance, M. (1992) *J. Magn. Reson. 96*, 6670−6678.
45. Ikura, M., Bax, A., Clore, G. M., and Groneborn, A. M. (1990) *J. Am. Chem. Soc. 112*, 9020−9022.
46. Wittekind, M., and Mueller, L. (1993) *J. Magn. Reson. B101*, 205−210.
47. Grzesiek, S., and Bax, A. (1992) *J. Am. Chem. Soc. 114*, 6291−6293.
48. Clore, G. M., Bax, A., Driscoll, P. C., Wingfield, P. T., and Gronenborn, A. M. (1990) *Biochemistry 29*, 8172−8184.
49. Bax, A., Clore, G. M., and Gronenborn, A. M. (1990) *J. Magn. Reson. 88*, 425−431.
50. Ikura, M., Kay, L. E., Tschudin, R., and Bax, A. (1990) *J. Magn. Reson. 86*, 204−209.
51. Muhandiram, D. R., Farrow, N. A., Xu, G.-Y., Smallcombe, S. H., and Kay, L. E. (1993) *J. Magn. Reson. B102*, 210−213.
52. Vuister, G. W., Clore, G. M., Gronenborn, A. M., Powers, R., Garrett, D. S., Tschudin, R., and Bax, A. (1993) *J. Magn. Reson. B101*, 210−213.
53. Bax, A., and Pochapsky, S. S. (1992) *J. Magn. Reson. 99*, 638−643.
54. Cohn, M., and Towsend, J. (1954) *Nature 173*, 1090−1091.
55. Carr, H. Y., and Purcell, E. M. (1954) *Phys. Rev. 94*, 630−638.
56. Mildvan, A. S., and Engle, J. L. (1972) *Methods Enzymol. 49D*, 322−359.
57. Mildvan, A. S., and Cohn, M. (1963) *Biochemistry 2*, 910−919.
58. Mildvan, A. S., and Cohn, M. (1966) *J. Biol. Chem. 241*, 1178−1193.
59. Serpersu, E. H., Shortle, D., and Mildvan, A. S. (1986) *Biochemistry 25*, 68−77.
60. Serpersu, E. H., Shortle, D., and Mildvan, A. S. (1987) *Biochemistry 26*, 1289−1300.
61. Weber, D. J., Serpersu, E. H., Shortle, D., and Mildvan, A. S. (1990) *Biochemistry 29*, 8632−8642.
62. Weber, D. J., Meeker, A. K., and Mildvan, A. S. (1991) *Biochemistry 30*, 6103−6114.
63. Reed, G. H., Cohn, M., and O'Sullivan, W. J. (1970) *J. Biol. Chem. 245*, 6547−6552.
64. Clore, G. M., and Gronenborn, A. M. (1993) *Determination of Structures of Larger Proteins in Solution by Three- and Four-dimensional Heteronuclear Magnetic Resonance Spectroscopy*, CRC Press, Boca Raton, FL.
65. Wuthrich, K. (1986) *NMR of Proteins and Nucleic Acids*, John Wiley, New York.
66. Drohat, A. C., Baldisseri, D. M., Rustandi, R. R., and Weber, D. J. (1998) *Biochemistry* (in press).
67. Lackmann, M., Rajasekariah, P., Iismaa, S. E., Jones, G., Cornish, C. J., Hu, S., Simpson, R. J., Moritz, R. L., and Geczy, C. L. (1993) *J. Immunol. 150*, 2981−2991.
68. Kube, E., Becker, T., Weber, K., and Gerke, V. (1992) *J. Biol. Chem. 267*, 14175−14182.
69. Baudier, J., and Cole, R. D. (1988) *J. Biol. Chem. 263*, 5876−5883.
70. Landar, A., Hall, T. L., Cornwall, E. H., Correia, J. J., Drohat, A. C., Weber, D. J., and Zimmer, D. B. (1997) *Biochim. Biophys. Acta 1343*, 117−129.
71. Mildvan, A. S., Granot, J., Smith, G. M., and Liebman, M. (1979) *Adv. Inorg. Biochem. 2*, 211−236.
72. Kemp, B. E., and Pearson, R. B. (1991) *Methods Enzymol. 200*, 121−134.
73. Verghese, G. M., Johnson, J. D., Vasulka, C., Haupt, D. M., Stumpo, D. J., and Blackshear, P. J. (1994) *J. Biol. Chem. 269*, 9361−9367.
74. Graff, J. M., Young, T. N., Johnson, J. D., and Blackshear, P. J. (1989) *J. Biol. Chem. 264*, 21818−21823.
75. McIlroy, B. K., Walters, J. D., Blackshear, P. J., and Johnson, J. D. (1991) *J. Biol. Chem. 266*, 4959−4964.
76. Graff, J. M., Rajan, R. R., Randall, R. R., Nairn, A. C., and Blackshear, P. J. (1991) *J. Biol. Chem. 266*, 14390−14398.
77. Schleiff, E., Schmitz, A., McIlhinney, R. A. J., Manenti, S., and Vergeres, G. (1996) *J. Biol. Chem. 271*, 26794−26802.
78. Rosenthal, H. E. (1967) *Anal. Biochem. 20*, 525−532.

BI972701N